Available online at www.sciencedirect.com
ScienceDirect
Ceramics International 35 (2009) 3259–3268
CERAMICS INTERNATIONAL
www.elsevier.com/locate/ceramint

Thermal conduction model of metal and ceramics

Yoshihiro Hirata *

Department of Advanced Nanostructured Materials Science and Technology, Kagoshima University, 1-21-40 Korimoto, Kagoshima 890-0065, Japan

Received 27 February 2009; received in revised form 24 April 2009; accepted 21 May 2009
Available online 18 June 2009

Abstract

A theoretical analysis of the thermal conductivity (κ_v) of metals and ceramics from their Young's modulus (E), atomic weight (M) and density (ρ) based on a harmonic oscillator model is presented. The κ_v value is expressed as $(A\sqrt{gN_0})^3\rho(E/M)^{3/2}/2$, where A is the maximum displacement of a harmonic oscillator and equals the mean free path of lattice vibration, g is the size factor ($g = s/r_0$, s: cross sectional area of atom acted by force applied, r_0 : distance between two atoms in equilibrium state), and N_0 is the Avogadro number. The $A\sqrt{g}$ value is proportional to ρ. The κ_v value of a metal is strongly dominated by the mean free path (A) and decreases when E increases as a consequence of the formation of partial covalent and ionic bond in metal bond. On the other hand, the mean free path of non-oxide and oxide ceramics becomes significantly small as compared with metals. The structure factor $\rho(E/M)^{3/2}$ contributes to increase κ_v. A good agreement was shown between the measured and calculated κ_v values in a wide range from 1 to 2310 J/smK.

Keywords: C. Thermal conductivity; C. Mechanical properties; E. Thermal applications

1. Introduction

Thermal conductivity is an important basic property of a material, which is used to design a structure of assembly of functional parts or to estimate a temperature gradient in the material at a given energy flux. Fortunately many measured thermal conductivities of metals and ceramics are available [1,2]. The reported values of the thermal conductivity at 300 K are distributed within a very wide range: 7.82 (Mn)–427 (Ag) J/smK for metals and 1.10 (pyrex glass)–2310 (diamond) J/smK for ceramics. The phonon (lattice vibration) of constituent atoms contributes to convey the thermal energy from a high temperature side to a low temperature side. However, little theoretical approach has been proposed to explain reasonably the 3-digit range of thermal conductivity. This paper applied a simple harmonic oscillator model for lattice vibration and succeeded in explaining the wide range of thermal conductivity of metal and ceramics. This paper contains (1) discussion of the relation between lattice vibration and thermal conductivity, (2) a thermal conduction model, (3) an analysis of measured thermal conductivity, (4) the influence of chemical bond on lattice vibration and (5) a quantitative representation of thermal conductivity of metal and ceramics. The definitions of notation in this paper are listed in Table 1.

2. Lattice vibration and thermal conductivity

Fig. 1 shows a harmonic oscillator with mass m and force constant k of spring. The force (F) applied to mass m is proportional to the displacement x. The corresponding Newton's equation is expressed by Eq. (1),

$$m\frac{dx^2}{dt^2} = -kx \tag{1}$$

The solution for Eq. (1) is given by Eq. (2),

$$x = A\sin\left(\sqrt{\frac{k}{m}}t\right) \tag{2}$$

where A is the amplitude (maximum displacement). Eq. (2) is derived for the initial condition of $x = 0$ at $t = 0$. The time dependence of displacement x is shown in Fig. 1. The angular velocity, ω, is equal to $(k/m)^{1/2}$ and related to frequency (f),

* Tel.: +81 99 285 8325; fax: +81 99 257 4742.
E-mail address: hirata@apc.kagoshima-u.ac.jp.

0272-8842/$36.00
doi:10.1016/j.ceramint.2009.05.026

Table 1
Definitions of notation.

m	Mass of atom
x	Displacement of harmonic oscillator
t	Time
k	Force constant of spring
A	Amplitude of harmonic oscillator (maximum displacement)
A_0	Amplitude of harmonic oscillator for Ag
ω	Angular velocity ($=\sqrt{k/m}$) of harmonic oscillator
f	Frequency of lattice vibration
v	Velocity of lattice vibration
λ	Wave length of lattice vibration
K	Kinetic energy of lattice vibration
U	Potential energy of lattice vibration
W	Total energy (K plus U)
ρ	Density of solid material
v_a	Atomic volume
I	Flux of energy input to solid material
κ	Thermal conductivity of solid material of 1 mol atoms
κ_v	Thermal conductivity of solid material of 1 m^3
α_v	Thermal diffusibility of solid material of 1 m^3
T	Temperature
L	Thickness of solid material
C	Specific heat of solid of 1 mol atoms
C_v	Specific heat of solid of 1 m^3
C_P	Specific heat of solid at 1 atm
ℓ	Mean free path of lattice vibration
M	Weight of 1 mol atoms
V	Molar volume of 1 mol atoms
N_0	Avogadro number
α	Thermal expansion coefficient of solid
β	Compressibility of solid
r_0	Distance between two atoms in equilibrium
r	Extended distance between two atoms
r_c	Radius of atom for covalent bond
ε	Strain of lattice ($=(r-r_0)/r_0 = x/r_0$)
σ	Stress applied to lattice
s	Cross sectional area of atom
F	Force applied to lattice
E	Young's modulus of solid
g	Ratio of s to r_0 (size factor)
g_0	Ratio of s to r_0 for Ag
G	$A^3(gN_0)^{3/2}/2$ for metal or ceramics
G_0	$A_0^3(g_0N_0)^{3/2}/2$ for Ag

wave length (λ) and velocity (v) by Eq. (3).

$$\omega = \sqrt{\frac{k}{m}} = 2\pi f = 2\pi\frac{v}{\lambda} \tag{3}$$

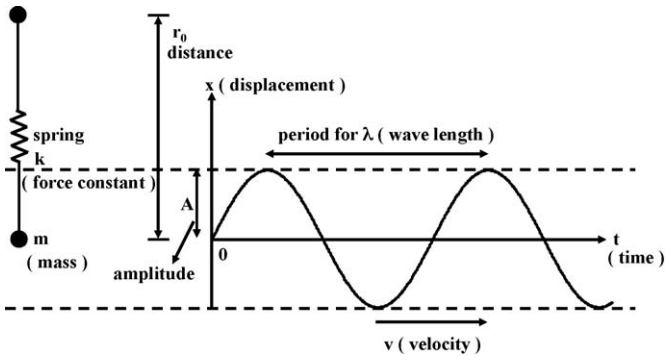

Fig. 1. Harmonic oscillator model of atom for lattice vibration.

Combination of Eqs. (2) and (3) gives the kinetic (K) and potential (U) energies of mass m by Eqs. (4) and (5), respectively [3].

$$K = \frac{1}{2}mv^2 = \frac{1}{2}m\left(\frac{dx}{dt}\right)^2 = \frac{1}{2}mA^2\omega^2\cos^2(\omega t) \tag{4}$$

$$U = \frac{1}{2}kx^2 = \frac{1}{2}mA^2\omega^2\sin^2(\omega t) \tag{5}$$

The total energy (W) becomes a constant value.

$$W = K + U = \frac{1}{2}mA^2\omega^2(\sin^2(\omega t) + \cos^2(\omega t)) = \frac{1}{2}mA^2\omega^2 \tag{6}$$

The density (ρ) of material containing atoms of mass m is equal to $\rho = m/v_a$, where v_a is atomic volume. For 1 m^3 of volume of material, the total energy is expressed by Eq. (7).

$$W = \frac{1}{2}\rho A^2\omega^2 \tag{7}$$

When the atom in Fig. 1 behaves as a harmonic oscillator, the total energy is conveyed at the velocity v. The flux (I) of energy conveyed per unit area (1 m^2) for unit time (1 s) is expressed by Eq. (8)

$$I = Wv = \frac{1}{2}\rho vA^2\omega^2 = \frac{1}{2}\rho\frac{k}{m}vA^2 \tag{8}$$

Eq. (8) indicates that the energy conveyed through a solid material depends both on the properties of material used ($\rho k/m$) and the wave produced by a harmonic oscillator (vA^2).

From Eq. (3), v is equal to $(\lambda/2\pi)(k/m)^{1/2}$. Furthermore, λ is equal to the length of circle of radius A, $2\pi A$ in Fig. 1. The substitution of these relations for Eq. (8) gives Eq. (9).

$$I = \frac{1}{2}\rho\frac{k}{m}vA^2 = \frac{1}{4\pi}\rho\left(\frac{k}{m}\right)^{3/2}\lambda A^2 = \frac{1}{2}\rho\left(\frac{k}{m}\right)^{3/2}A^3 \tag{9}$$

The energy conveyed in a solid material becomes larger under the following conditions: (1) high density (ρ) material, (2) large force constant (k) of spring (strong chemical bond), (3) low mass (m) of atom, (4) high velocity (v) of wave, (5) long wave length (λ), and (6) large amplitude (A, large displacement of harmonic oscillator). The flux of energy is related to thermal conductivity in the next section.

3. Thermal conductivity

Thermal conductivity (κ) is defined by Eq. (10),

$$I = \kappa\frac{dT}{dL} \tag{10}$$

where dT/dL represents a temperature gradient along one direction of material. The flux of energy conveyed is proportional to κ value at a constant temperature gradient. For a constant I value, a high κ value leads to a small temperature difference. An opposite case is caused for a low κ value. The κ

value is related to the properties of material by Eq. (11),

$$\kappa = \frac{1}{3} C \ell v \tag{11}$$

where C (J/K mol) is the specific heat of 1 mol atoms of solid, ℓ the mean free path by lattice vibration and v the velocity of wave. This equation is discussed more in a latter part of this section. The specific heat, C, is theoretically derived as a function of temperature by Einstein and Debye [4], and approaches a constant value of $3R$ (R: gas constant, 8.314 J/K mol) with increasing temperature. Since the density (ρ) of 1 mol atoms is equal to M/V (M: atomic weight, V: molar volume of atoms), C is converted to a specific heat per unit volume, C_v (J/Km^3) as follows: $C_v = C\rho/M$. That is, the thermal conductivity per unit volume (κ_v, J/smK) is expressed by Eq. (12),

$$\kappa_v = \frac{1}{3} C_v \ell v = \left(\frac{1}{3}\frac{\rho}{M} C\right) \ell v \tag{12}$$

The flux of energy conveyed by a harmonic oscillator in solid material of 1 m^3 (Eq. (9)) is compared with Eqs. (10) and (12) at an unit temperature difference ($\Delta T = 1$ K) along unit distance ($\Delta L = 1$ m).

$$I = \left(\frac{1}{2}\rho\frac{k}{m}\right) v A^2 = \kappa_v = \left(\frac{1}{3}\frac{\rho}{M} C\right) \ell v \tag{13}$$

Eq. (13) leads to the relation expressed by Eq. (14),

$$\left(\frac{1}{2}\frac{kN_0}{mN_0}\right) A^2 = \left(\frac{1}{2}\frac{kN_0}{M}\right) A^2 = \left(\frac{1}{3}\frac{C}{M}\right) \ell \tag{14}$$

where N_0 is the Avogadro number. From the relation expressed by Eq. (14), we obtain the following interesting information.

$$A = \ell \tag{15}$$

$$\frac{1}{2}(kN_0)A = \frac{1}{3} C \tag{16}$$

The amplitude A in Fig. 1 (maximum displacement) corresponds to the mean free path of a wave by lattice vibration. The force applied to a spring of force constant k, to extend the bonding distance between two atoms to $A/2$ along one direction, is equal to 1/3 of C (specific heat along one direction). Since the C value in Eq. (16) approaches $3R$ at a high temperature, A value becomes larger at a smaller k value (weak chemical bond). Eqs. (3), (15) and (16) are substituted for Eq. (12) to understand the influence of C_v, ℓ and v on κ_v.

$$\kappa_v = \frac{1}{3} C_v \ell v = \frac{1}{3}\left(\frac{\rho}{M} C\right)\left(\frac{2}{3} C \frac{1}{kN_0}\right)\left(\frac{2}{3} C \frac{1}{N_0}\sqrt{\frac{1}{mk}}\right) = \frac{4}{27}\left(\frac{C}{\sqrt{MkN_0}}\right)^3 \rho \tag{17}$$

A decrease of force constant k enhances the mean free path and velocity of the wave. Similarly, a decrease of atomic weight of the material increases the C_v and v values. The above tendency contributes to increase κ_v. As a result, Eq. (17) provides a simple form of κ_v as functions of the properties of material (C, M, k and ρ).

The product of ℓv is experimentally measured as a thermal diffusibility α_v (m^2/s). The measurement of C_v of solid is difficult as compared with the measurement of C_P at a constant pressure. Eq. (18) provides the relation between C_P and C_v,

$$C_P = C_v + \frac{\alpha^2 V T}{\beta} \tag{18}$$

where α is the thermal expansion coefficient, β the compressibility, V the molar volume and T the temperature. Although α, β and C_P are as a function of temperature, the difference of $C_P - C_v$ can be negligible below 800 K [4]. Therefore, the measured C_P may be used as C_v in Eq. (17). The κ_v is determined experimentally from α_v and C_P, and has a physical meaning expressed by Eq. (17).

4. Thermal conduction model

The factors affecting κ_v were analyzed in the previous section. However, Eq. (17) still contains the k value which is difficult to evaluate experimentally. The k value is approximated by Young's modulus (E) as follows. Fig. 1 shows a force applied to atom ($F = -kx$). The strain (ε) in chemical bond of atom, produced by a harmonic oscillator, is expressed by Eq. (19),

$$\varepsilon = \frac{r - r_0}{r_0} = \frac{x}{r_0} \tag{19}$$

where r_0 ($\gg x$) is the distance between two atoms in an equilibrium state and r the extended distance. The Young's modulus is defined by Eq. (20),

$$E = \frac{\sigma}{\varepsilon} = \frac{F/s}{\varepsilon} = \frac{r_0 F}{sx} = \frac{r_0 kx}{sx} = \frac{r_0 k}{s} \tag{20}$$

where σ is the stress applied and equal to F/s (s: the cross sectional area of atom acted by force applied). The Young's modulus is directly related to the force constant and distance between two atoms. An open structure giving a large distance (r_0) leads to the increased E value at a similar s value. The relation derived from Eq. (20), $k = gE$ ($g = s/r_0$), is substituted for Eq. (9) to analyze the effects of mean free path and the product of $\rho(E/M)^{3/2}$ on the thermal conductivity.

$$\kappa_v = \frac{1}{2} A^3 (gN_0)^{3/2} \rho \left(\frac{E}{M}\right)^{3/2} \tag{21}$$

On the other hand, the atomic volume (v_a) in material is expressed by Eq. (22),

$$v_a = \frac{M}{N_0 \rho} \tag{22}$$

Substitution of Eq. (22) for Eq. (21) gives Eq. (23), which is expressed as functions of E, M, and V ($=v_a N_0$, molar volume of material).

$$\kappa_v = \frac{2}{1} A^3 (gN_0)^{3/2} \frac{E^{3/2}}{VM^{1/2}} \tag{23}$$

Eqs. (21) and (23) indicate that the increase in E and ρ and decrease in M and V are effective to increase κ_v. However, an opposite effect is induced in A value when E value increases (Eq. (16)). Increased E reduces A value, resulting in the decrease of κ_v. Both the effects of E and A were investigated with the reported data of κ_v for metal and ceramics in the next section.

5. Analysis of measured thermal conductivity of metal and ceramics

Fig. 2 shows the relation between $\log \kappa_v$ at 300 K and $\log \rho(E/M)^{3/2}$ based on Eq. (21). The data for polycrystalline metal and single or polycrystalline ceramics were cited mainly from chemical handbook [1]. For ceramic materials, average atomic weight (M (average)) was used in Eq. (21): M (average) = M' (molecular weight)/$N_0(x+y)$ for binary composition of A_xB_y. Similarly, an average molar volume, V ($=v_aN_0$), was calculated by M' (molecular weight)/$\rho\,(x+y)$. The each straight line in Fig. 2 was drawn with a slope 1. The good linearity is well explained by the proposed relation in Eq. (21). The κ_v values of metal, non-oxide ceramics and oxide ceramics are proportional to the product of $\rho(E/M)^{3/2}$ (named as structure factor in this paper). The structure factor is in 3-digit range. The intercept in Fig. 2 at $\rho(E/M)^{3/2} = 1$ represents $A^3(gN_0)^{3/2}/2$ and g is named as size factor. Increase in A means the decrease of k in Eq. (16), resulting in the decrease of g ($=s/r_0$) or E in Eq. (20). For metal, g value may be treated as a similar value because of the limited structures of metal (body-centered cubic, hexagonal or cubic close packing). In this case, the intercept reflects mainly the influence of A value. As shown in Fig. 2, a metal has a variety of A and $\left(A\sqrt{gN_0}\right)^3/2$ value changes in 2-digit range. The measured κ_v values are located at least on 7 lines (a–h). The line a has the highest A value and the line h has the lowest A value. In other words, the metal on line a has the relatively small force constant of chemical bond and the metal on line h has a relatively large force constant of chemical bond.

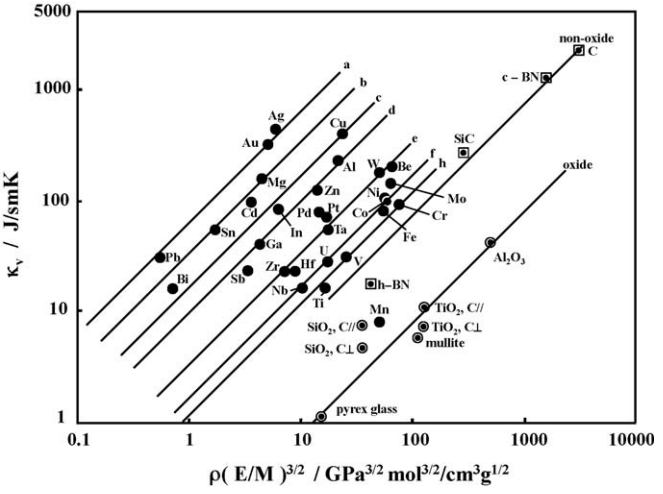

Fig. 2. Relation between $\log \kappa_v$ (thermal conductivity) and $\log \rho(E/M)^{3/2}$ (ρ: density, E: Young's modulus, M: atomic weight) for metal and ceramics at 300 K.

In ceramic materials, the intercept of κ_v line, $\left(A\sqrt{gN_0}\right)^3/2$ value in Eq. (20), occurs at lower values. Ceramic materials have generally larger E values than metals because of the increased fraction of covalent bond or ionic bond. This change in E (large force constant) decreases A value, causing the decrease of the intercept of κ_v line. The effect of A value may be more significant for oxide ceramics than for non-oxide ceramics. Oxide ceramics have relatively a higher fraction of ionic bond rather than covalent bond. On the other hand, non-oxide ceramics, typically like diamond, have a high fraction of covalent bond. The above interpretation leads to the conclusions that (1) the intercept of κ_v line in Fig. 2 is closely related to the product of $\left(A\sqrt{g}\right)^3$, (2) a large variety of intercept of metal reflects mainly the difference of A value, (3) a large A value is related to a small force constant (k) of chemical bond, (4) ceramic materials have lower A values because of the larger force constant (or larger Young's modulus), and (5) the influence of ionic bond is significant than covalent bond in ceramic materials for the decrease of thermal conductivity.

The above conclusions explain the two typical κ_v values of Ag and diamond as follows: Ag has the highest A value (the lowest force constant) and the significantly large mean free path contributes to the large κ_v value. Diamond has a low A values (a large force constant) but the structure factor ($\rho(E/M)^{3/2}$) becomes highest because of the highest force constant. This large structure factor contributes to the highest κ_v value. In the next section, we analyze the relation between A value and chemical bond in metal.

6. Influence of chemical bond on lattice vibration of a metal

As seen in Fig. 2, metal has a large variety of structure factor and A value. To understand systematically the κ_v value, we introduce a concept of ideal metal which has the same A and g values as Ag (Fig. 3). For Ag, the thermal conductivity is expressed by Eq. (24),

$$\kappa_v(Ag) = \frac{1}{2}A_0^3(g_0N_0)^{3/2}\rho_{Ag}\left(\frac{E}{M}\right)_{Ag}^{3/2} \tag{24}$$

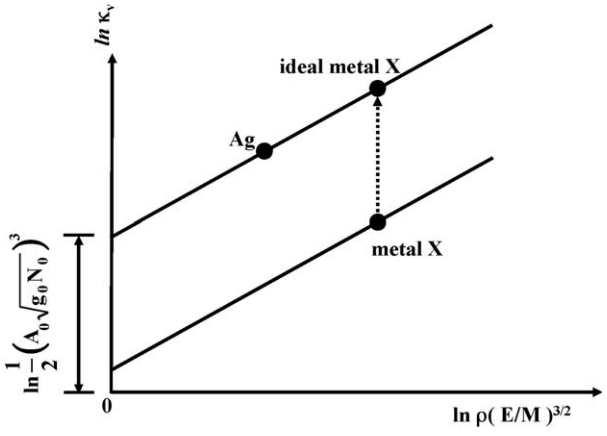

Fig. 3. $\log \kappa_v - \log \rho(E/M)^{3/2}$ relation for ideal metal with the same $A\sqrt{g}$ value as Ag (A: mean free path, g: size factor ($=s/r_0$, s: cross sectional area of atom acted by force applied, r_0: distance between two atoms in equilibrium state).

where A_0 and g_0 are mean free path and size factor for Ag. From Fig. 2, we know the value of product of $(A_0\sqrt{gN_0})^3/2$ (named as G_0). The κ_v for metal x and ideal metal x are expressed by Eqs. (25) and (26), respectively.

$$\kappa_v(x) = \frac{1}{2}A^3(gN_0)^{3/2}\rho_x\left(\frac{E}{M}\right)_x^{3/2} \tag{25}$$

$$\kappa_v(ix) = \frac{1}{2}A_0{}^3(g_0N_0)^{3/2}\rho_x\left(\frac{E}{M}\right)_x^{3/2} \tag{26}$$

The ratio of κ_v $(x)/\kappa_v$ (ix) is given by Eq. (27).

$$\frac{\kappa_v(x)}{\kappa_v(ix)} = \frac{(1/2)A^3(gN_0)^{3/2}}{(1/2)A_0^3(g_0N_0)^{3/2}} = \frac{G}{G_0} = \left(\frac{A\sqrt{g}}{A_0\sqrt{g_0}}\right)^3 \tag{27}$$

When $\sqrt{g}$ is a similar value to $\sqrt{g_0}$, A/A_0 ratio is approximated to $(G/G_0)^{1/3}$. Therefore, we know A/A_0 ratio from G/G_0 ratio. The factors affecting A/A_0 ratio are analyzed with available physical or chemical parameters.

6.1. Ionization energy

The ionization in metal structure may produce partial ionic bond in metal bond because of the charge neutrality ($X \rightarrow X^+ + X^-$). The formation of ionic bond produces the difference in size of atom (small cation and large anion). A repulsive interaction is produced between the ions of X^+–X^+ and X^-–X^-. On the other hand, X^+ and X^- ions are attracted by an electrostatic force. The above interaction between metal ions may affect the positions of atoms in metal. As a result, the mean free path of metal is reduced like ceramic materials in Fig. 2. Fig. 4 shows the relation between $A\sqrt{g}/A_0\sqrt{g_0}$ ratio and 1st ionization energy for metal with $\rho(E/M)^{3/2}$ of 0.6–77 $GPa^{3/2}$ $mol^{3/2}$ cm^{-3} $g^{-1/2}$. In the following description, the condition of $\sqrt{g}/\sqrt{g_0} \approx 1$ is assumed to make clear discussion. The decrease of ionization energy reduces A/A_0 ratio of metal with a structure factor of 10–17 or 51–60 $GPa^{3/2}$ $mol^{3/2}$ cm^{-3} $g^{-1/2}$. This tendency is explained well by the formation of partial ionic bond in metal. However, the A/A_0 ratio increases in the low ionization energy range below 720 kJ/mol. This phenomenon may be related to the contribution of electrons at the Fermi surface and is discussed in a latter part. The metal with a relatively small structure factor of 0.6–9 $GPa^{3/2}$ $mol^{3/2}$ cm^{-3} $g^{-1/2}$ gives the relatively high A/A_0 ratios. This result is explained by the decreased force constant of chemical bond (Young's modulus) as shown in Eq. (16). However, the A/A_0 ratio shows a complicated change as a function of ionization energy and drops drastically at 720 kJ/mol of ionization energy.

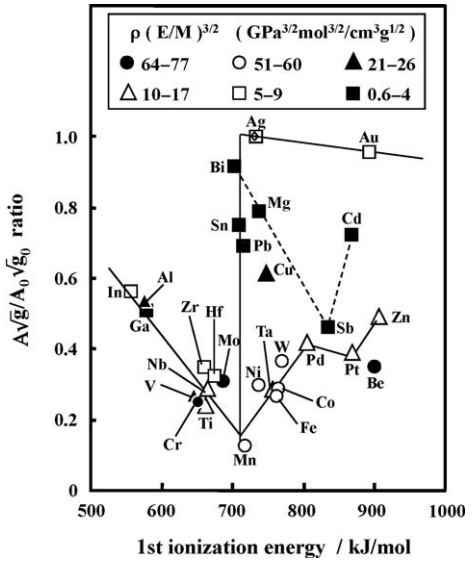

Fig. 4. Influence of first ionization energy on $A\sqrt{g}/A_0\sqrt{g_0}$ ratio of metal (A_0: mean free path of lattice vibration for Ag, g_0: size factor for Ag).

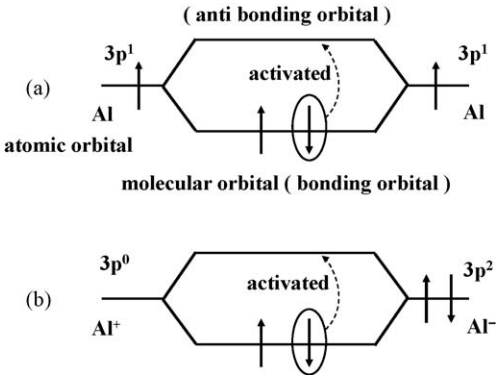

Fig. 5. Relation between atomic orbital and molecular orbital for (a) two Al atoms and (b) Al^+–Al^- ions.

In the low ionization energy range (<720 kJ/mol), the A/A_0 ratio increases again. The mean free path by lattice vibration decreases drastically at around 720 kJ/mol of ionization energy, leading to the decrease of κ_v. The decreased κ_v enhances the temperature gradient between a high temperature side and a low temperature side at a given flux of energy (Eq. (10)). The thermal energy input at a high temperature side accelerates the jump of electrons at the Fermi surface to the conduction band. The simple molecular orbital model for two Al atoms is shown in Fig. 5. The electrons activated to the conduction band move to the low temperature side and this movement conveys the input energy as kinetic energy of electrons. In the metal of a high ionization energy, most of the input energy is conveyed by lattice vibration.

6.2. Features of metal bond

From the characteristic of κ_v in Fig. 2, the A value decreases in the following order of chemical bond: metal bond > covalent bond (non-oxide ceramics) > ionic bond (oxide ceramics). The complicated behavior of A/A_0 ratio of metal with a low structure factor in Fig. 4 is understood by the localization of electrons in metal bond. In the ideal metal bond, electrons are delocalized in the structure, producing non-directional chemical bond. This structure is achieved by the bond of s atomic orbital, leading to the spherical structure model of metal atom. The localization of electrons in p, d or f orbital produces the directional chemical bond. The chemical bond with p, d or f orbital is not effective to make smooth lattice vibration (non-directional chemical bond).

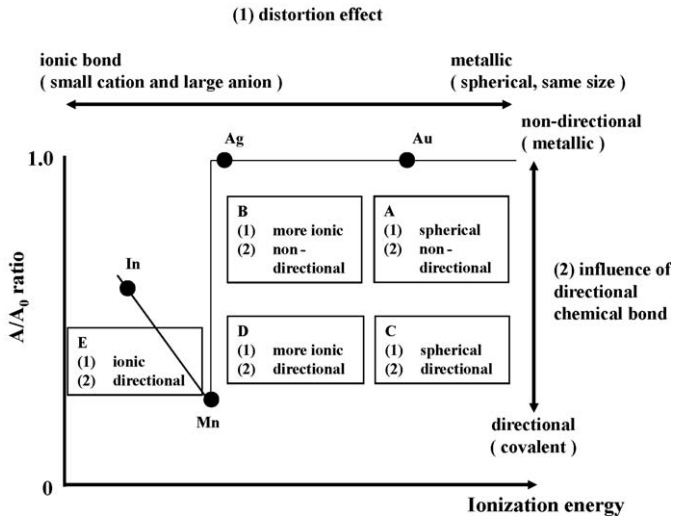

Fig. 6. Schematic feature of metal bond evaluated with A/A_0 ratio and first ionization energy.

ρ (E/M)$^{3/2}$ (GPa$^{3/2}$ mol$^{3/2}$/cm^{3}g$^{1/2}$)	Lines in Fig. 2	Type
0.6–4	b–d	II
5–9	a	I
10–80	d–h	III

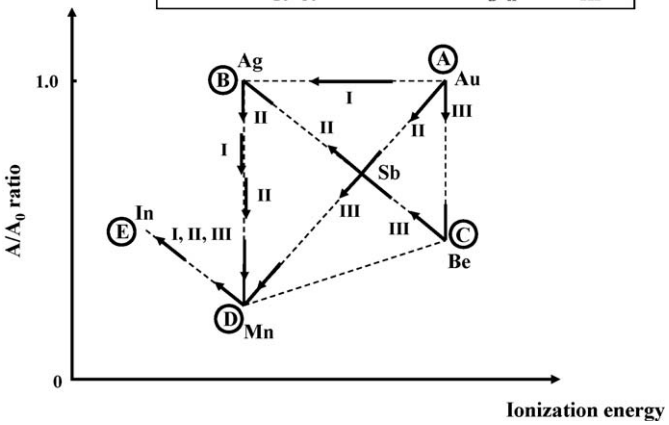

Fig. 7. Change in A/A_0 ratio with ionization energy for three types of metal with different $\rho(E/M)$ ratio.

This type of covalent bond is mixed in metal bond. Further localization of electrons produces partial ionic bond.

Fig. 6 shows the schematic features of metal bond evaluated from (1) the distortion effect (introduction of ionic bond) and (2) directional chemical bond (introduction of covalent bond of p, d or f orbital). Region A represents the ideal non-directional metal bond with spherical atoms of same size. A typical metal in region A is Au and whose ground sate electron configuration is 4f ^{14}5d^{10}6s^1. Inside 4f and 5d orbitals are completely occupied by 14 and 10 electrons, respectively. Only spherical 6s^1 orbital contributes effectively to form metal bond. In region B, more ionic property may be added to metal bond. A typical metal in region B is Ag. The ground state electron configuration of Ag is 4d^{10}5s^1. Only 5s^1 orbital of Ag is used to form metal bond. Other metal with s^1 orbital is Cu. The ground state electron configuration of Cu is 3d^{10}4s^1. As seen in Fig. 4, Cu also provides the relatively high A/A_0 ratio. In region C, covalent bond of metal with p, d or f orbital increases, resulting in the decreased A/A_0 ratio. The typical metal in region C is Be with ground state electron configuration of 1s^{2}2s^2. The metal bond is formed by sp^1 hybrid orbital using two electrons of 2s^2. The shape of sp^1 hybrid orbital provides the strong directional bond. This characteristics leads to the decrease of A/A_0 ratio. The metal in region D contains both ionic bond and covalent bond in addition to metal bond. The mean free path is greatly decreased by this structural feature. In Fig. 4, Mn is a typical metal in region D. Its ground state electron configuration is 3d^{5}4s^2. The d orbital of Mn is used to form strong directional chemical bond. In region E, the lattice vibration is greatly disturbed by the introduction of ionic bond and covalent bond. In region E, the electrons activated to the conduction band may contribute to convey the input energy as discussed in Section 6.1.

When Au, Ag, Be, Mn and In are located at the each corner in Fig. 7, the change of A/A_0 ratio with ionization energy is divided in typical three types. The A/A_0 ratio of metal in group I with a structure factor 5–9 GPa$^{3/2}$ mol$^{3/2}$ cm^{-3}g$^{-1/2}$ changes along A → B → D → E with decreasing ionization energy. The A/A_0 ratio of group II with a small structure factor of 0.6–4 GPa$^{3/2}$ mol$^{3/2}$ cm^{-3} g$^{-1/2}$ changes along the path of A → Sb → B → D → E with decreasing ionization energy. Sb or Pd is located in the center of the trapezoid in Fig. 7. The mean free path of other metal with a large structure factor above 10 GPa$^{3/2}$ mol$^{3/2}$ cm^{-3} g$^{-1/2}$ changes along A → C → Sb → D → E. The A/A_0 ratio is strongly dominated by the mixing fraction of metal, covalent and ionic bond and structure factor. It is noted that Mg (3s^2), Cd (4d^{10}5s^2), Zn (3d^{10}4s^2) and Pd (4p^{6}4d^{10}) have no vacant atomic orbital. The magnitude of A/A_0 ratio in Fig. 4 decreases in the following order: s^1 orbital (Au, Ag, Cu) > completely occupied orbital (Mg, Cd, Zn, Pd) > d orbital (Mn, Ta, V, Ti). In Section 7, we discuss more another important factor affecting the A/A_0 ratio.

6.3. Effect of Young's modulus

In Section 6.2, it is understood that the characteristics of metal bond affects the mean free path of lattice vibration. As shown in Eq. (21), another factors included in κ_v are ρ, E and M. In this section, we discuss the $(E/M)^{3/2}$ value. Fig. 8 shows the relation $(E/M)^{3/2}$ and v_a (atomic volume). Each metal contains different fractions of metal, ionic and covalent bond and has a different crystal structure. In Fig. 8, v_a was calculated by $4\pi r_c^3/3$, where r_c is the reported radius of atom for covalent bond [5]. In Fig. 8, some data for ceramic materials are also included. The high E/M ratio means the large normalized force constant (k/m) and long distance between atoms (r_0) as indicated by Eq. (20). The reported $(E/M)^{3/2}$ value is distributed in 3-digit range. For a similar $(E/M)^{3/2}$ value, two different v_a values are plotted. As a result, two curves are drawn. Both the lines show the decrease of $(E/M)^{3/2}$ value with increasing v_a value. That is, the increased atomic volume leads to the decrease of normalized force constant but may increase the distance between atoms. The two lines (a and b) give a wide $(E/M)^{3/2}$ value range at a similar v_a. This distribution of normalized E value represents the feature of chemical bond of

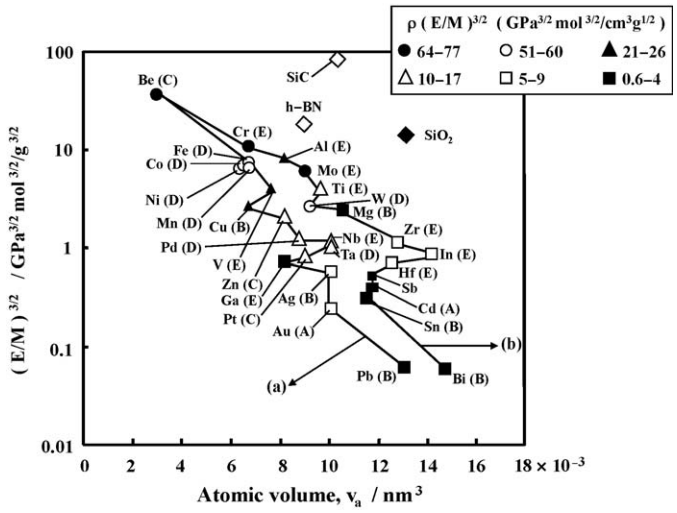

Fig. 8. $(E/M)^{3/2}$ value and atomic volume calculated with radius of atom for covalent bond. The category of *A–E* indicates the feature of metal shown in Fig. 6. The center of the label is Sb in Fig. 7.

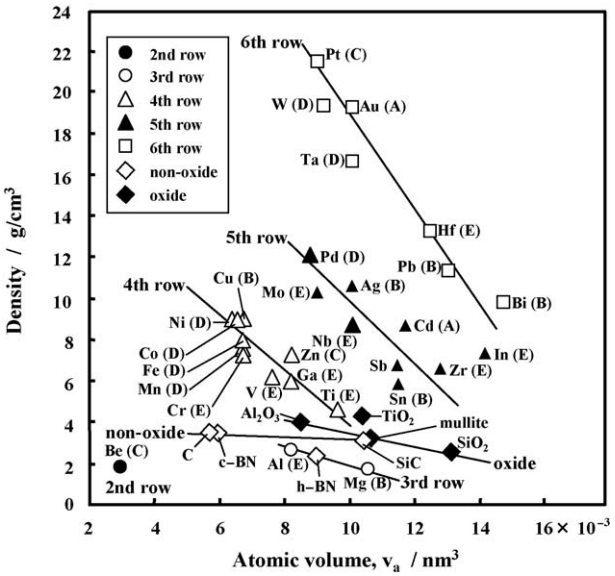

Fig. 9. Density of metal as a function of atomic volume. The category of *A–E* indicates the feature of metal shown in Fig. 6.

metal. The line (a) contains C and D metal with high covalent bond in Figs. 4 and 6. On the other hand, line (b) contains *E* metal with a low ionization energy (<720 kJ/mol). Metal A and B are observed on both the lines. The above observation indicates (1) line (a) represents the atomic size dependence of normalized force constant of metal with strong covalent bond and (2) line (b) corresponds to the atomic size dependence of normalized force constant of metal with strong covalent and ionic bond, and (3) the force constant becomes larger when ionic bond is added to the mixture of metal–covalent bond at a similar atomic size. Some data for ceramic materials are plotted in Fig. 8. The ceramic materials with strong covalent or ionic bond give high $(E/M)^{3/2}$ values as compared with metals. That is, introduction of covalent bond or ionic bond to a metal bond increases the force constant (Young's modulus). As seen in Figs. 5, 6 and 8, the characteristics of chemical bond affect both the mean free path and normalized Young's modulus.

6.4. Effect of density

Fig. 9 shows the density of metal as a function of v_a. In Fig. 9, densities of non-oxide and oxide ceramic materials are also plotted against the average atomic volume. The density of metal at a same row in the periodic table of elements decreases linearly with an increase of v_a. This tendency is repeated periodically. The increased number of the row enhances the density because of the increased atomic number. However, in one row, no clear relation is observed between the order of the density and atomic number. The density of metal in one row decreases as follows: D (>C, A) > B, E of metal labeled in Figs. 4 and 6. The introduction of covalent bond to metal bond causes the increase of density. This tendency may be explained by the increased force constant as discussed in Section 6.3. On the other hand, introduction of ionic bond to metal decreases the density as compared with the influence of covalent bond. That is, the influence of directional chemical bond in a metal is greater than the distortion effect by ionic bond in Fig. 6 on the density of the metal. The interesting observation is the good linearity of density as a function of v_a. The feature of chemical bond changes from metal–covalent bond to metal–covalent–ionic bond with increasing atomic volume. This change of chemical bond is directly reflected in the density of a metal. The density of ceramic materials is relatively smaller than that of metals. The density of oxide with ionic and covalent bond decreases at a larger average atomic volume. In the ionic bond-rich oxide, lager O^{2-} ions are close packed. Smaller cations are located at the spaces between O^{2-} ions. On the other hand, non-oxide ceramics with covalent bond have strong directional chemical bond, giving an open structure. The above feature provides a larger dependence of density on the atomic volume for ionic bond-rich ceramics. The good linearity of the density$-v_a$ relation for ceramics also indicates that the density reflects the continuous change of chemical bond with increasing atomic volume.

7. Representation of thermal conductivity of metal and ceramics

7.1. Metal

In Section 5, the important factors affecting the thermal conductivity were discussed. In this section, representation of a thermal conductivity with available parameters is constructed. From Eq. (27), the following relation is derived.

$$G = G_0 \left(\frac{A\sqrt{g}}{A_0\sqrt{g_0}} \right)^3 \tag{28}$$

Eq. (28) is substituted for Eq. (25) to obtain Eq. (29).

$$\kappa_v(x) = G_0 \left(\frac{A\sqrt{g}}{A_0\sqrt{g_0}} \right)^3 \rho_x \left(\frac{E}{M} \right)_x^{3/2} \tag{29}$$

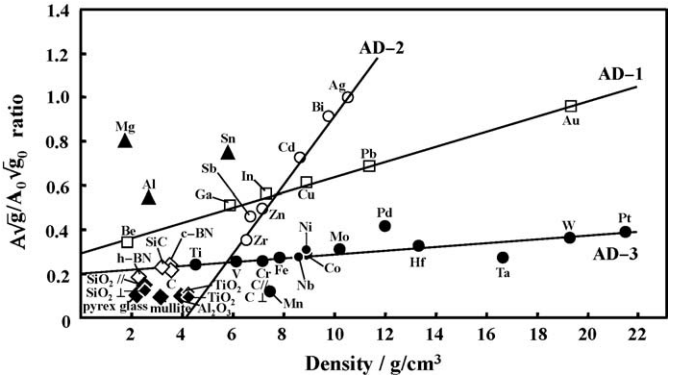

Fig. 10. Density dependence of $A\sqrt{g}/A_0\sqrt{g_0}$ ratio for metal and ceramics.

The data of ρ, E and M are easily available in chemical or metal handbook. The G_0 value is determined from Eq. (24) for Ag. The final issue is to represent the $A\sqrt{g}/A_0\sqrt{g_0}$ ratio with available properties of material. The $A\sqrt{g}/A_0\sqrt{g_0}$ ratio shown in Figs. 4 and 6 is greatly influenced by the nature of chemical bond. After several parameters of material were investigated, a very good linear relation was found between the $A\sqrt{g}/A_0\sqrt{g_0}$ ratio and density of metal. Fig. 10 shows the density dependence of $A\sqrt{g}/A_0\sqrt{g_0}$ ratio for metal and ceramics. As seen in Fig. 10, three linear lines can represent the $A\sqrt{g}/A_0\sqrt{g_0}$−density relation of many kinds of metals. The theoretical derivation of the linear relation is presented in Section 7.3. Both the factors of A and density can express the continuous change of chemical bond of metal as discussed previously. The three lines in Fig. 10 are named as AD-1, AD-2 and AD-3, respectively. AD-1 line includes Au, Pb, Cu, In, Ga, and Be. AD-2 line with a large slope includes Ag, Bi, Cd, Zn, Sb and Zr. The other metal is located on AD-3 line with a small slope. The metal included in each line is well understood by analyzing the relation in Fig. 8. Fig. 11 shows again the $(E/M)^{3/2}-v_a$ relation. The metal on AD-1 line has the lowest

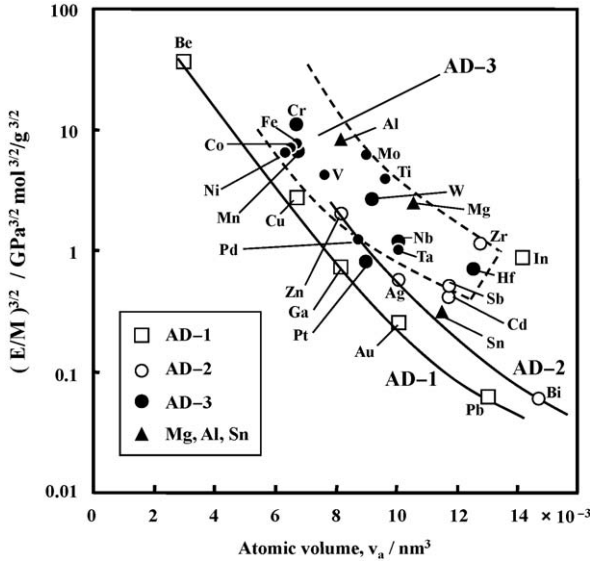

Fig. 11. $(E/M)^{3/2}-v_a$ (atomic volume) relation for metal associated three AD-lines in Fig. 10.

$(E/M)^{3/2}$ value (small force constant) at a similar v_a value. The metal on AD-2 line has a secondary low $(E/M)^{3/2}$value at a given v_a. The metal on AD-3 line has a relatively large $(E/M)^{3/2}$value (large force constant). The AD line in Fig. 10 is reflected to the $(E/M)^{3/2}-v_a$ curve in Fig. 11. The good linear relation in Fig. 10 was coupled with Eq. (29) to represent κ_v with ρ, E and M.

$$\kappa_v(\text{AD-1}) = 72.545\rho\left(\frac{E}{M}\right)^{3/2}(0.03441\rho + 0.2997)^3 \tag{30}$$

$$\kappa_v(\text{AD-2}) = 72.545\rho\left(\frac{E}{M}\right)^{3/2}(0.1547\rho - 0.6140)^3 \tag{31}$$

$$\kappa_v(\text{AD-3}) = 72.545\rho\left(\frac{E}{M}\right)^{3/2}(0.008473\rho + 0.2071)^3 \tag{32}$$

The unit of parameters in Eqs. (30), (31) and (32) are follows: $[\kappa_v]$ = [J/smK], [E] = [GPa], [M] = [atomic weight/mol]. A coefficient of correlation for AD-1, AD-2 and AD-3 lines in Fig. 10 was 0.9989, 0.9943 and 0.9783, respectively.

7.2. $A\sqrt{g}$ value of Mg, Al and Sn

As seen in Fig. 10, Mg, Al and Sn are far from AD lines and show the relative high $A\sqrt{g}/A_0\sqrt{g_0}$ ratios at a low density range (<6 g/cm³). This result is characterized by the $(E/M)^{3/2}-v_a$ relation in Fig. 11. Mg and Al have the relatively high $(E/M)^{3/2}$ values as compared with the metals on AD-1 and AD-2 lines. The magnitude of $(E/M)^{3/2}$ of Mg and Al is comparable to that of metal with a large normalized force constant on AD-3 line. However, their $A\sqrt{g}/A_0\sqrt{g_0}$ ratios are larger than those of metal on AD-3 line. From Eqs. (16) and (20), Eq. (33) is derived.

$$gA\left(\frac{E}{M}\right) = \frac{2}{3}\frac{C}{MN_0} \tag{33}$$

The product of $gA(E/M)$ becomes a constant value at a grain atomic weight. A large (E/M) ratio gives a small gA product. However, $A\sqrt{g}$ is a function of $\sqrt{g}$ as shown by Eq. (34).

$$(A\sqrt{g})\left(\frac{E}{M}\right) = \left(\frac{2}{3}\frac{C}{N_0}\right)\frac{1}{M\sqrt{g}} \tag{34}$$

A large (E/M) ratio and a large $A\sqrt{g}$ value for Mg and Al can be explained by the decrease of $M\sqrt{g}$. Since g is the ratio of s/r_0 and M is related to density (ρ) by Eq. (22), $M\sqrt{g}$ is expressed by Eq. (35).

$$M\sqrt{g} = (v_a\rho N_0)\sqrt{\frac{s}{r_0}} = \left(\frac{4}{3}\pi^{3/2}N_0\right)\rho r_c^4\frac{1}{\sqrt{r_0}} \tag{35}$$

The v_a (atomic volume) and s (cross sectional area) of atom are expressed by $4\pi {r_c}^3/3$ and πr_c^2 (r_c: radius of atom for covalent bond), respectively. The decrease of $M\sqrt{g}$ is related to the decrease of ρ and r_c and the increase of r_0. As seen in Fig. 9, the r_c (v_a) values of Mg and Al are comparable to those of other metal on AD-3 line. However, densities for both Mg and Al are

significantly small. That is, the decrease of $M\sqrt{g}$ is associated with the small density of Mg and Al. Therefore, AD-3 line for the metal with a relatively large $(E/M)^{3/2}$ value goes up from Ti to Mg through Al with decreasing density owing to the $M\sqrt{g}$ effect.

On the other hand, the $(E/M)^{3/2}$ value of Sn is located on AD-2 line in Fig. 11 and small. A relatively small $(E/M)^{3/2}$ value indicates a large gA value for Sn. The $A\sqrt{g}$ value for Sn is also increased by the small $M\sqrt{g}$ value. Basically the behavior of Sn in Figs. 10 and 11 is interpreted based on AD-2 line. The AD-2 line goes up from Zr to Sn owing to the decrease of density, which increases the $A\sqrt{g}$ value as explained by Eqs. (34) and (35).

The combination of Eqs. (22), (34) and (35) can explain the linear relation between $A\sqrt{g}$ and density in Fig. 10.

$$A\sqrt{g} = \frac{2}{3}\frac{C}{N_0 E\sqrt{g}} = \left(\frac{2}{3}\frac{Cv_a}{ME}\sqrt{\frac{r_0}{s}}\right)\rho \tag{36}$$

Eq. (36) provides a linear relation between $A\sqrt{g}$ and ρ when the $Cv_a\sqrt{r_0}/ME\sqrt{s}$ value is treated as a constant value. Fig. 10 suggests that the $Cv_a\sqrt{r_0}/ME\sqrt{s}$ value can be approximated to the slope of AD-1, AD-2 or AD-3 line. However, the $Cv_a\sqrt{r_0}/ME\sqrt{s}$ value of Mg, Al or Sn is to be determined from the slope of line connecting the origin and $A\sqrt{g}/A_0\sqrt{g_0}$ ratio at a given density in Fig. 10. For Mg and Al, the $Cv_a\sqrt{r_0}/ME\sqrt{s}$ value becomes significantly larger than the other metal on AD-3 line.

7.3. Ceramics

The $A\sqrt{g}/A_0\sqrt{g_0}$ ratios of non-oxide and oxide ceramics are shown in Fig. 10. The ratios (~0.23) fore non-oxide are very close to AD-3 line of metal. That is, it is possible to interpret that non-oxide ceramics is the extrapolated structure of metal on AD-3 line with a large force constant in the low density range. The $A\sqrt{g}/A_0\sqrt{g_0}$ ratios of oxide enriched with covalent and ionic bond are low values (~0.11) and almost independent of density below 4 g/cm^3. That is, the mean free path of oxide is about 1/10 of that of Ag. In ceramic materials, the density dependence of $A\sqrt{g}/A_0\sqrt{g_0}$ ratio is small and κ_v values of non-oxide and oxide are expressed by Eqs. (37) and (38), respectively.

$$\kappa_v(\text{non-oxide}) = 72.545\rho\left(\frac{E}{M}\right)^{3/2}(0.2288)^3 \tag{37}$$

$$\kappa_v(\text{oxide}) = 72.545\rho\left(\frac{E}{M}\right)^{3/2}(0.1122)^3 \tag{38}$$

The thermal conductivity of ceramics is dominated by density and Young's modulus, and the $A\sqrt{g}$ value of lattice vibration can be treated as a constant value.

7.4. Comparison of measured and calculated thermal conductivities

Fig. 12 shows the measured and calculated κ_v values in the range from 1 to 2310 J/smK. The measured κ_v values of metal

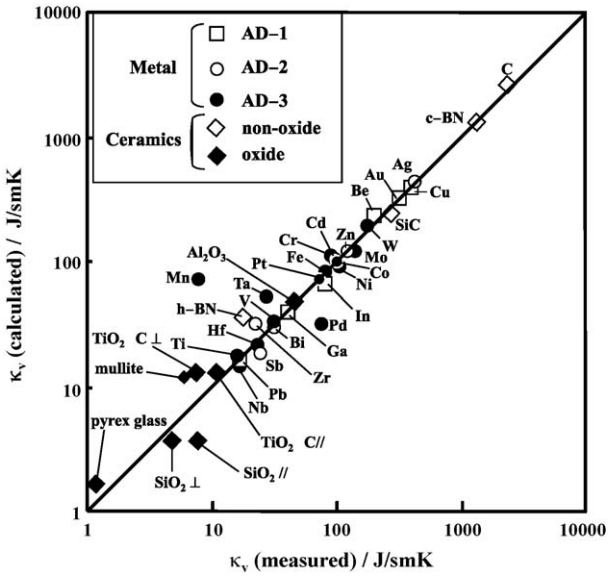

Fig. 12. Comparison between measured and calculated κ_v values for metal and ceramics.

on AD-1 and AD-2 lines are well represented by Eqs. (30) and (31), respectively. A relatively large difference of κ_v values is observed for Pd, Ta and Mn on AD-3 line. The deviation of the $A\sqrt{g}/A_0\sqrt{g_0}$ ratio from AD-3 line is responsible for the observed difference of κ_v in Fig. 12. The measured κ_v values of non-oxide and oxide ceramics are also well represented by Eqs. (37) and (38), respectively. Based on the good agreement between the measured and calculated κ_v values, it is interesting to see the measured κ_v values as a function of density.The measured κ_v in Fig. 13 has a large variety at a low density region and the width of κ_v becomes narrow as the density increases. The 1st spike of κ_v in the density range of 2–4 g/cm^3 is produced by the combination of the high κ_v of non-oxide ceramics and the low κ_v of oxide ceramics. The κ_v values of metal are located between the spike. The high κ_v of non-oxide

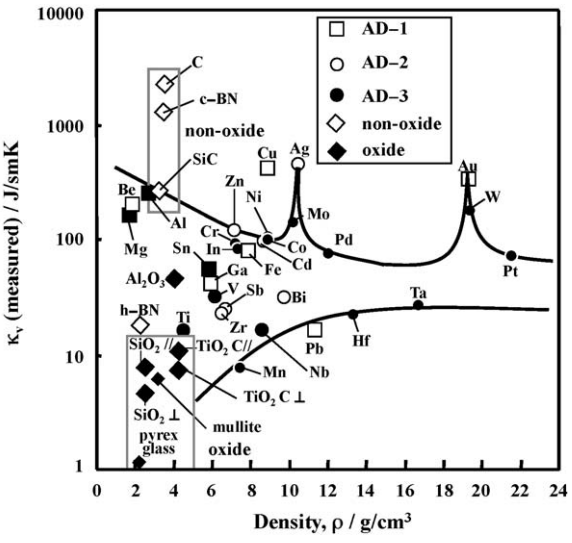

Fig. 13. Density dependence of κ_v of metal and ceramics.

ceramics is due to the high $(E/M)^{3/2}$ ratio in Eq. (21). On the other hand, the low κ_v of oxide ceramics originates from the low $A\sqrt{g}$ value (Fig. 10). The width of κ_v of metal is mainly related to the $(E/M)^{3/2}$ ratio. The upper line, which decreases with increasing density, is associated with the decrease of $(E/M)^{3/2}$ ratio for the metal with the highest density at each row (Al, Ni, Co, Pd, and Pt in Figs. 9 and 11). The lower line, which increases with increasing density is explained by the increased $(E/M)^{3/2}$ ratio and density of 6th row metal (Pb, Hf and Ta in Figs. 9 and 11). The second spike at Cu reflects the high $A\sqrt{g}$ value and relatively high $(E/M)^{3/2}$ ratio (Figs. 9 and 10). The high κ_v value of Ag is explained by the highest $A\sqrt{g}$ value and the intermediate density. The third spike at Au is related to the high $A\sqrt{g}$ value and the high density for Au. The high density and relatively high $(E/M)^{3/2}$ ratio for W contributes to the increased κ value.

8. Conclusions

The thermal conductivity (κ_v) of metals and ceramics depends basically on the mean free path (A) of lattice vibration, density (ρ) and normalized Young's modulus (E/M, M: atomic weight): $\kappa_v = (A\sqrt{gN_0})^3 \rho (E/M)^{3/2}/2$, where g is the size factor ($g = s/r_0$, s: cross sectional area of atom acted by force applied, r_0: distance between two atoms in an equilibrium state) and N_0 the Avogadro number. The $A\sqrt{g}$ value is also proportional to ρ. Both ρ and E values are closely related to the nature of chemical bond of metal and ceramics. The nature of chemical bond of metal is divided into three types based on the normalized Young's modulus: weak chemical bond at a given atomic volume (Au, Pb, Cu, In, Ga, Be, AD-1 line in Fig. 10), intermediate chemical bond (Ag, Bi, Cd, Zn, Sb, Zr, AD-2 line), strong chemical bond (Pt, W, Ta, Hf, Pd, Mo, Ni, Co, Nb, Fe, Cr, V, Ti, AD-3 line). Addition of covalent bond to metal bond enhances the force constant of chemical bond. Further mixing of ionic bond to metal–covalent bond increases more the strength of chemical bond. The increased strength of chemical bond, which is accompanied by the decrease of density in each group of metals, reduces the mean free path of lattice vibration, resulting in the decrease of κ_v. Generally, the κ_v of metals increases as the density increases at a similar (E/M) ratio. An exceptional increased mean free path is observed for low density Mg, Al and Sn. In these types of metal, $M\sqrt{g}$ value is significantly small and the $A\sqrt{g}$ value is increased by the $M\sqrt{g}$ effect (Eq. (34) in text). As a result, Mg, Al and Sn provide relatively high κ_v value. On the other hand, the thermal conductivity of ceramics is dominated by density and normalized Young's modulus because the $A\sqrt{g}$ value of lattice vibration can be treated as a constant value. In ceramics, the chemical bond is strengthened more than in metals by the formation of covalent and ionic bond. The increased strength of chemical bond of ceramics reduces drastically the mean free path of lattice vibrations. The density dependence of $A\sqrt{g}$ value is small in a narrow density range ($2 < \rho < 4$ g/cm^3). The highest κ_v of diamond can be explained by the highest $\rho\ (E/M)^{3/2}$ value. A very good agreement was shown between the measured κ_v values (1–2310 J/smK) and calculated κ_v for metal and ceramics.

References

[1] K. Hata (Ed.), Chemical Handbook, Basic Part II, third edition, The Chemical Society of Japan, Maruzen, Tokyo, 1984, pp. 73–74.
[2] S. Nagasaki (Ed.), Metal Handbook, second edition, The Japan Institute of Metals, Maruzen, Tokyo, 1984, pp. 12–15.
[3] D.A. McQuarrie, Quantum Chemistry, Univ. Science Books, Mill Valley, CA, USA, 1983, pp. 153–158.
[4] R.A. Swalin, Thermodynamics of Solids, second edition, John Wiley & Sons, New York, 1972, pp. 28–31, 53–62.
[5] J.D. Lee, A New Concise Inorganic Chemistry, third edition, Van Nostrand Reinhold Co, Ltd., Berkshire, 1977(translated to Japanese by H. Hamaguchi and H. Kanno, Tokyo Kagaku Dojin, Tokyo, 1982, p. 94).